Mechanism of covalency-induced electric polarization within the framework of maximally localized Wannier orbitals

Kiyoyuki Terakura[1,2,3] and Shoji Ishibashi[1,4]

[1]*Nanomaterials Research Institute, AIST, Umezono, Tsukuba, Ibaraki 305-8568, Japan*

[2]*National Institute for Materials Science, Sengen, Tsukuba, Ibaraki 305-0047, Japan*

[3]*Japan Advanced Institute of Science and Technology, Nomi, Ishikawa 923-1292, Japan*

[4]*JST, CREST, Tokyo 102-0076, Japan*

(Received 22 November 2014; revised manuscript received 4 April 2015; published 13 May 2015)

It has been well established that covalency significantly enhances the electric polarization produced by the ionic displacement for ferroelectric perovskite transition metal oxides (TMO). Furthermore, recent experimental and theoretical works on the organic ferroelectrics TTF-CA (tetrathiafulvalene-*p*-chloranil) have revealed that the covalency-induced polarization is one to two orders of magnitude larger than that of the ionic polarization and that the two contributions are in the *opposite* direction. Here we propose a formulation to analyze the detailed mechanism of the covalency-induced polarization within the framework of maximally localized Wannier orbitals and apply it to an organic exotic ferroelectrics TTF-CA and typical ferroelectric perovskite TMOs, $BaTiO_3$, and $PbTiO_3$. This formulation discriminates three components in the electronic contribution to the polarization. The first one corresponds to the point charge model, the second to the intra-atomic or molecular polarization, and the third comes from the electron transfer between unit cells. The framework of the present formulation is the same as the one proposed by Bhattacharjee and Waghmare [Phys. Chem. Chem. Phys. **12**, 1564 (2010)], but we give a more explicit expression of each component and discuss fundamental aspects of the formulation.

DOI: 10.1103/PhysRevB.91.195120 PACS number(s): 71.20.−b, 77.84.−s

I. INTRODUCTION

Since the seminal work on the theory of the electric polarization in solids [1,2], remarkable progress has been achieved in our understanding of dielectric properties of various kinds of materials [3]. The perovskite-type transition-metal oxides (TMO) are the most popular materials in this regard. Based on the analysis of Born effective charges, an important concept of the covalency-enhanced polarization has been established [4–8]. The electronic contribution to the electric polarization induced by covalency has the same sign and the same order of magnitude as the one caused by the displacement of ions in the point charge model (PCM). For example, the Born effective charges of Ti and $O_{||}$ in $BaTiO_3$ are 6 to 7 and about −5 with $O_{||}$ denoting the oxygen atom forming a pair with Ti in the ferroelectric phase (see Table 4 in Ref. [3]). The mechanism of covalency-induced polarization for perovskites has been explained from various viewpoints [8]. In particular, it was shown that Harrison's interpretation based on his bond-order model [9] gives semiquantitative results for the Born effective charge of $O_{||}$ and that the electron transfer between the nearest Ti atoms of the $O_{||}$ plays an important role. The band-by-band decomposition [8,10,11] clarified in each valence band the contribution from each orbital to the Born effective charge giving qualitative support to Harrison's interpretation. In addition to these works, a formal decomposition of the Born effective charge into fundamental electronic processes was made by Bhattacharjee and Waghmare [12] within the framework of a maximally localized Wannier orbital (MLWO) [13].

In the present work we adopt the same approach as the one of Ref. [12] and give more explicit expressions to three types of the electronic contribution to the electric polarization and discuss some fundamental aspects of the formulation. In the process of deriving the final expression, we first obtain four contributions which are characterized by the point charge displacement, the intra-atomic or molecular polarization, the electron transfer between atoms in a unit cell, and the electron flow from cell to cell. However, it will be shown that the third and fourth contributions are mutually convertible depending on the choice of the unit cell and the basis vectors in the unit cell, while the sum of the two is well defined. We point out that the contribution from the electron transfer within a unit cell should not exist in a periodic bulk system. Therefore, we convert the third term to a part of the fourth term and finally obtain three contributions to the polarization.

In order to demonstrate how the formulation works, we apply it to an organic ferroelectrics TTF-CA (tetrathiafulvalene-*p*-chloranil) and the perovskite TMOs, $BaTiO_3$, and $PbTiO_3$. The former is an exotic ferroelectric material in which the electronic contribution to the polarization is more than 20 times larger than the ionic polarization and the two contributions are in the *opposite* direction [14]. As TTF-CA has a strong one-dimensional character, the application of our formulation is straightforward and clear. The analysis of the unique aspects of TTF-CA has been published in our previous paper [15] and some additional results and supplementary discussions will be given in the present work. The analysis is extended to the three-dimensional material $BaTiO_3$ [16] and $PbTiO_3$. For these materials we discuss the actual charge state (not the formal valence) of each element and the detailed mechanism of the covalency-induced electric polarization.

As the main aim of the present work is to propose a formulation for analyzing the electronic processes in the polarization and demonstrate it as a useful tool, we do not pursue accuracy and efficiency of the calculation and neglect some terms which will make only marginal contributions,

although actual numerical calculations based on Berry's phase were done with higher accuracy. The organization of the present paper is as follows. We describe our formulation in Sec. II and explain the mechanism of the polarization in Sec. III. The details of the numerical calculations are described in Sec. IV and the formulation is applied to TTF-CA, $BaTiO_3$, and $PbTiO_3$ in Sec. V. We conclude in Sec. VI.

II. FORMULATION

In this section we describe the formulation for a general case. The framework of our formulation is the same as the one of Ref. [12]. Applications of the formulation to specific cases TTF-CA, $BaTiO_3$, and $PbTiO_3$ will be made in the later sections. We start with the expression for the electronic polarization in terms of the Wannier function centers (WFC) and then give an expression for the total polarization including contributions from nuclei and core electrons. A simpler version of the formulation was described in our recent work [16] where only the O-2p bands were considered as the valence bands of $BaTiO_3$ and the detailed derivation of the expression for the polarization was not given.

A. Electronic contribution

We consider a general case in which some different bunches of valence bands make non-negligible contributions to the polarization. For example, O-2s, O-2p, Pb-5d, and Pb-6s bands correspond possibly to these valence bands, among which O-2p and Pb-6s bands in $PbTiO_3$ are essential. The number of band branches belonging to the jth bunch of valence bands is denoted as n_{v_j}. In order to discuss the contribution from each bunch of valence bands using the WFC, we have to treat each bunch of valence bands separately, because only the total WFC is gauge invariant [13]. In the following formulation we pick up one particular bunch of valence bands, say the jth bunch as an example and derive an expression for the polarization of the band(s) in terms of four basic physical processes. The total polarization is given by summing up the polarization thus obtained over j. In the following, the index j is mostly not shown explicitly unless confusion is unavoidable.

We convert the Bloch functions $\psi^{\lambda}_{m\vec{k}}(\vec{r})$ of the n_v valence bands to the corresponding MLWOs with the following equation:

$$a^{\lambda}_{nl}(\vec{r}) = \frac{1}{\sqrt{N}} \sum_{\vec{k}} e^{-i\vec{k}\cdot\vec{R}_l} \sum_{m=1}^{n_v} \psi^{\lambda}_{m\vec{k}}(\vec{r}) W^{\vec{k},\lambda}_{m,n}, \tag{1}$$

where N is the number of unit cells in the system with the periodic boundary condition, n is the orbital index of MLWO, m is the band index, $\vec{k}$ is the wave vector in the first Brillouin zone, $\vec{R}_l$ is the position of the lth unit cell, and $W^{\vec{k},\lambda}_{m,n}$ is the unitary matrix to convert the Bloch functions to MLWO. The superscript λ denotes the linear interpolation parameter for the polarization with $\lambda = 0$ the paraelectric phase and $\lambda = 1$ the ferroelectric phase. These MLWOs are of the bonding-state type and the nth branch WFC is defined by

$$\vec{r}^{\,\lambda}_n = \int \vec{r}\, \left|a^{\lambda}_{nl=0}(\vec{r})\right|^2 d\vec{r}. \tag{2}$$

Then the electronic polarization produced by the n_v occupied bands is given by

$$\Delta \vec{P}^1_{\rm el} = \frac{-2e}{\Omega} \Delta \vec{r}^{\,1}, \tag{3}$$

where the suffix "el" denotes the electronic contribution to the electric polarization, $-e$ is the electronic charge, the factor 2 is the spin degeneracy, Ω is the unit cell volume, and $\Delta\vec{r}^{\,\lambda}$ is the total shift of WFC given by

$$\Delta \vec{r}^{\,\lambda} = \sum_{n=1}^{n_v} \Delta \vec{r}^{\,\lambda}_n = \sum_{n=1}^{n_v} \left(\vec{r}^{\,\lambda}_n - \vec{r}^{\,0}_n\right). \tag{4}$$

The λ dependencies of lattice constants and Ω are small and neglected in the present formulation though included in the actual numerical calculations for the polarization in terms of Berry's phase and for MLWOs. Similarly to Ref. [12], we define another set of MLWOs from n_{vc} bands which covers all the bunches of valence bands considered and the bottom n_c conduction bands with the following equation:

$$\phi^{\lambda}_{tl}(\vec{r}) = \frac{1}{\sqrt{N}} \sum_{\vec{k}} e^{-i\vec{k}\cdot\vec{R}_l} \sum_{m=1}^{n_{vc}} \psi^{\lambda}_{m\vec{k}}(\vec{r}) U^{\vec{k},\lambda}_{m,t}, \tag{5}$$

with t ranging from 1 to n_{vc}. In the above equation we define

$$n_{vc} = \sum_j n_{v_j} + n_c. \tag{6}$$

The suffix t represents both the atom (or molecule) specified by i and its orbitals specified by ξ. These MLWOs $\phi^{\lambda}_{tl}(\vec{r})$ correspond to the occupied atomic (or molecular) orbitals or unoccupied atomic (or molecular) orbitals of the atoms (or molecules) forming the lth unit cell. Physically we expect that these MLWOs constitute a set of localized orbitals and that the bonding type and antibonding type combinations among them form $\sum_j n_{v_j}$ valence bands and n_c conduction bands.

With these preparations, we expand the valence band MLWO of Eq. (1) belonging to the unit cell at the origin as a linear combination of the basis set MLWOs of Eq. (5) as follows:

$$a^{\lambda}_n(\vec{r}) = a^{\lambda}_{nl=0}(\vec{r}) = \sum_l \sum_{t=1}^{n_{vc}} C^{\lambda}_{n,tl} \phi^{\lambda}_{tl}(\vec{r}). \tag{7}$$

The expansion coefficient $C^{\lambda}_{n,tl}$ can be expressed in terms of the unitary matrices W and U in Eqs. (1) and (5) as

$$C^{\lambda}_{n,tl} = \frac{1}{N} \sum_{\vec{k}} e^{i\vec{k}\cdot\vec{R}_l} \sum_{m=1}^{n_v} W^{\vec{k},\lambda}_{m,n} U^{\vec{k},\lambda *}_{m,t}. \tag{8}$$

The completeness of the expansion Eq. (7) is guaranteed by

$$\sum_l \sum_{t=1}^{n_{vc}} \left|C^{\lambda}_{n,tl}\right|^2 = \frac{1}{N} \sum_{\vec{k}} \sum_{m=1}^{n_v} W^{\vec{k},\lambda *}_{m,n} W^{\vec{k},\lambda}_{m,n} = 1. \tag{9}$$

In the following we treat all the quantities in Eq. (7) to be real because of the empirical fact that MLWOs are real [13]. Inserting Eq. (7) into Eq. (2) we obtain

$$\vec{r}^{\,\lambda}_n = \sum_{t,l} \sum_{t',l'} C^{\lambda}_{n,tl} C^{\lambda}_{n,t'l'} \int \vec{r}\, \phi^{\lambda}_{tl}(\vec{r}) \phi^{\lambda}_{t'l'}(\vec{r}) d\vec{r}. \tag{10}$$

第l个超包等于原包

We introduce an explicit form of $\phi^{\lambda}_{il}(\vec{r})$ as

$$\phi^{\lambda}_{i\xi l}(\vec{r}) = \phi^{\lambda}_{i\xi}(\vec{r} - \lambda\vec{\tau}_i - \vec{b}_i - \vec{R}_l), \tag{11}$$

where we use the atom index i and the orbital index ξ explicitly instead of the suffix t, $\vec{\tau}_i$ and $\vec{b}_i$ denote the ferroelectric displacement and the basis vector of an atom i in a unit cell. With Eq. (11), the WFC of Eq. (10) is written as

$$\begin{aligned}\vec{r}^{\,\lambda}_n = &\sum_{i,\xi,l} \left(C^{\lambda}_{n,i\xi l}\right)^2 (\lambda\vec{\tau}_i + \vec{b}_i + \vec{R}_l) \\ &+ \sum_i \sum_{\xi,\xi'} \left\{ \sum_l C^{\lambda}_{n,i\xi l} C^{\lambda}_{n,i\xi' l} \right\} \int \vec{r}\,\phi^{\lambda}_{i\xi}(\vec{r})\phi^{\lambda}_{i\xi'}(\vec{r})d\vec{r} \\ &+ \text{other terms},\end{aligned} \tag{12}$$

where we have made use of the orthonormality relation of MLWO ϕ^{λ}_{il}. The "other terms" includes the $\vec{r}$ weighted integrals of the MLWO overlap between different sites which can be numerically estimated using Eqs. (43) and (44) of Ref. [17]. These integrals are only of the order of 10^{-3} Å in the case of TTF-CA but can be as large as 0.05 Å in $BaTiO_3$ and $PbTiO_3$. However, with the corresponding occupation matrix elements [with an extension of Eq. (18) to the site off-diagonal case] of the order of 0.1, these other terms with an assumption of ten additive contributions produce polarization of at most about 1.0 μC/cm^2. This amount of contribution cannot be totally neglected but is only a few percent of the observed polarization of these materials. Therefore, we neglect the other terms in this work. To obtain the polarization [Eq. (3)], we have to sum $\vec{r}^{\,\lambda}_n$ over n. The summation of the first term of Eq. (12) over n is given by

$$\begin{aligned}&\sum_{n=1}^{n_v} \sum_{i,\xi,l} \left(C^{\lambda}_{n,i\xi l}\right)^2 (\lambda\vec{\tau}_i + \vec{b}_i + \vec{R}_l) \\ &= \sum_i \left\{ \sum_{\xi} \sum_{l} \sum_{n=1}^{n_v} \left(C^{\lambda}_{n,i\xi l}\right)^2 \right\} (\lambda\vec{\tau}_i + \vec{b}_i) \\ &\quad + \sum_l \left\{ \sum_i \sum_{\xi} \sum_{n=1}^{n_v} \left(C^{\lambda}_{n,i\xi l}\right)^2 \right\} \vec{R}_l.\end{aligned} \tag{13}$$

Similarly, for the summation of the second term of Eq. (12) over n, we obtain

$$\sum_i \sum_{\xi,\xi'} \left\{ \sum_l \sum_n C^{\lambda}_{n,i\xi l} C^{\lambda}_{n,i\xi' l} \right\} \int \vec{r}\,\phi^{\lambda}_{i\xi}(\vec{r})\phi^{\lambda}_{i\xi'}(\vec{r})d\vec{r}. \tag{14}$$

Hereafter we use the renormalized coefficients defined by

$$c^{\lambda}_{n,i\xi l} = \sqrt{2} C^{\lambda}_{n,i\xi l}, \tag{15}$$

in order to absorb the spin degeneracy factor 2 in Eq. (3). We further define the following quantities:

$$\left(c^{\lambda}_{i\xi l}\right)^2 = \sum_{n=1}^{n_v} \left(c^{\lambda}_{n,i\xi l}\right)^2, \tag{16}$$

$$\left(c^{\lambda}_{il}\right)^2 = \sum_{\xi} \left(c^{\lambda}_{i\xi l}\right)^2, \tag{17}$$

the occupation matrix

$$w^{\lambda}_{i,\xi\xi'} = \sum_l \sum_{n=1}^{n_v} c^{\lambda}_{n,i\xi l} c^{\lambda}_{n,i\xi' l}, \tag{18}$$

its diagonal element being the number of valence electrons in the orbital specified by i and ξ,

$$w^{\lambda}_{i\xi} = w^{\lambda}_{i,\xi\xi}, \tag{19}$$

and the number of valence electrons of the atom i,

$$w^{\lambda}_i = \sum_{\xi} w^{\lambda}_{i\xi} = \sum_l \left(c^{\lambda}_{il}\right)^2. \tag{20}$$

Then using the completeness relation of Eq. (9), we obtain

$$\sum_i w^{\lambda}_i = 2n_v. \tag{21}$$

The matrix element in Eq. (14) is the intra-atomic (or molecular) dipole tensor given by

$$\vec{d}^{\lambda}_{i,\xi'\xi} = \int \vec{r}\,\phi^{\lambda}_{i\xi'}(\vec{r})\phi^{\lambda}_{i\xi}(\vec{r})d\vec{r}, \tag{22}$$

where the origin of $\vec{r}$ is taken at the position of the atom i. With the quantities defined above, the polarization is given by

$$\begin{aligned}\Delta\vec{P}^1_{\rm el} = \frac{-e}{\Omega} \sum_i \Bigg[&w^1_i \vec{\tau}_i + \sum_{\xi\xi'} w^1_{i,\xi\xi'} \vec{d}^{\,1}_{i,\xi'\xi} \\ &+ \Delta w^1_i \vec{b}_i + \sum_l \Delta\left(c^1_{il}\right)^2 \vec{R}_l \Bigg],\end{aligned} \tag{23}$$

where we define for every quantity A,

$$\Delta A^{\lambda} = A^{\lambda} - A^0. \tag{24}$$

In the second term of Eq. (23) we do not have to subtract the corresponding quantity for $\lambda = 0$, because in the system with the inversion symmetry such a contribution should vanish even if some atoms may have nonzero intra-atomic dipole tensor. Due to the sum rules of Eqs. (9) and (21) the following relations hold:

$$\sum_l \sum_i \sum_{\xi} \Delta\left(c^{\lambda}_{i\xi l}\right)^2 = \sum_l \sum_i \Delta\left(c^{\lambda}_{il}\right)^2 = 0, \tag{25}$$

$$\sum_i \Delta w^{\lambda}_i = 0. \tag{26}$$

Equation (23) is an expression for the electronic contribution to the polarization and corresponds to Eq. (11) of Ref. [12]. Our formulation has a more explicit expression of each contribution.

The first term of Eq. (23) corresponds to PCM and the second term comes from the intra-atomic (or molecular) polarization, which we call the local polarization (LP) hereafter. If every atom has basis orbitals belonging to the same inversion symmetry property (parity), all the components of intra-atomic dipole tensors vanish. In the paraelectric phase, due to the inversion symmetry of the system, this statement holds exactly. On the other hand, it is only approximately true in the ferroelectric phase [18]. Even if some atoms or

molecules may have basis orbitals with different parity and have local polarization, the total polarization will vanish in the paraelectric phase. However, in such cases, the local polarization can make significant contribution to the total polarization in the ferroelectric phase. The third term is the polarization due to the electron transfer between atoms in a unit cell. The first three terms in Eq. (23) are related to electron density distribution (EDD). In contrast to them, the fourth term is totally independent from EDD. In fact, this term represents the *charge transfer between cells* [19] which we call the electron flow (EF) and does not induce any changes in EDD as can be easily understood by considering the periodic array of the bonding-state MLWOs.

We make comments on the dependence of each term of Eq. (23) on the choice of the unit cell. As long as we estimate the polarization given by Eqs. (3) and (4) by following continuously along the adiabatic parameter λ, $\Delta\vec{P}_{\rm el}$ of Eq. (23) and its first two terms are independent of the choice of the unit cell. On the other hand, the basis vectors $\vec{b}_i$ of the third term depend on the choice of the unit cell. However, to make $\Delta\vec{P}_{\rm el}$ invariant, the sum of the third and fourth terms is independent of the choice of the unit cell. More importantly, the electron transfer between atoms in a unit cell should not contribute to the polarization in the periodic bulk system. Otherwise it produces a macroscopic electric field in the system similar to the problem of polar catastrophe [20], which is in contradiction to the basic situation in the modern theory of the polarization [21]. This consideration is also consistent with the fact that the electric polarization estimated by the charge density distribution in a unit cell vanishes after taking the average over the possible position of the unit cell origin [21]. Therefore, we merge the third and fourth terms into a modified electron-flow contribution as described below.

For this purpose we first calculate the polarization for $\lambda = -1$ similar to that for $\lambda = 1$ and obtain

$$\Delta\vec{P}^{-1}_{\rm el} = \frac{-e}{\Omega}\sum_i \left[-w_i^{-1}\vec{\tau}_i + \sum_{\xi\xi'} w^{-1}_{i,\xi\xi'}\vec{d}^{-1}_{i,\xi'\xi} + \Delta w_i^{-1}\vec{b}_i + \sum_l \Delta\left(c^{-1}_{il}\right)^2 \vec{R}_l \right]. \tag{27}$$

Note that the sign of the first term changes because of the opposite direction of the displacement of atoms. The coefficient $c^{-1}_{n,i\xi l}$ can be related to $c^{1}_{n,i\xi l}$ by using the inversion symmetry relation as explicitly shown in the Supplemental Material [22]. The following relations hold:

$$w^{-1}_{i,\xi\xi'} = s_{i\xi}s_{i\xi'}w^1_{i,\xi\xi'} \tag{28}$$

and

$$\vec{d}^{-1}_{i,\xi'\xi} = -s_{i\xi}s_{i\xi'}\vec{d}^1_{i,\xi'\xi}, \tag{29}$$

where $s_{i\xi}$ denotes the parity of the orbital specified by $(i\xi)$ and takes $+1$ for even parity and -1 for odd parity. Therefore, we obtain

$$\Delta\vec{P}^{-1}_{\rm el} = \frac{-e}{\Omega}\sum_i \left[-w_i^{1}\vec{\tau}_i - \sum_{\xi\xi'} w^{1}_{i,\xi\xi'}\vec{d}^{1}_{i,\xi'\xi} + \Delta w_i^{1}\vec{b}_i + \sum_l \Delta\left(c^{-1}_{il}\right)^2 \vec{R}_l \right]. \tag{30}$$

The first two terms of this equation are just minus those of Eq. (23) while the third term is the same as the corresponding one of Eq. (23). The fourth term is modified from that in Eq. (23) so that the sum of the third and fourth terms is just minus the sum of the corresponding two terms of Eq. (23), as is proved in the Supplemental Material [22]. Therefore, as expected, we have the relation

$$\Delta\vec{P}^{-1}_{\rm el} = -\Delta\vec{P}^{1}_{\rm el}. \tag{31}$$

Now we can obtain the following expression for the polarization by taking the difference between Eqs. (23) and (30) and dividing the difference by two:

$$\Delta\vec{P}_{\rm el} = \frac{-e}{\Omega}\sum_i \left[w_i^{1}\vec{\tau}_i + \sum_{\xi\xi'} w^{1}_{i,\xi\xi'}\vec{d}^{1}_{i,\xi'\xi} + \sum_l \Delta\left(\tilde{c}_{il}\right)^2 \vec{R}_l \right]. \tag{32}$$

This expression does not have the third term of Eq. (23) and the coefficients in the electron-flow term are modified as

$$\Delta(\tilde{c}_{il})^2 = \tfrac{1}{2}\left[\Delta\left(c^{1}_{il}\right)^2 - \Delta\left(c^{-1}_{il}\right)^2\right]. \tag{33}$$

B. Total polarization

In order to give an explicit expression for the total polarization, we estimate the contributions from the rest of the system including a nucleus and core electrons to the Born effective charge Z_i for atom i. With the contribution from the jth bunch of bands to Z_i denoted as Z_i^j, the contribution from the rest of the system is given by

$$Z_i^r = Z_i - \sum_j Z_i^j. \tag{34}$$

Z_i^r is well treated as a point charge if even deep semicore states are treated as valence states, and the polarization by its displacement can be combined with the first term of Eq. (32). The local charge of the atom i is given by

$$q_i = Z_i^r - \sum_j w_i^{j,1}, \tag{35}$$

where the superscript j in the second term shows explicitly the contribution from the jth bunch of bands. Then the total polarization is given by

$$\Delta\vec{P} = \frac{e}{\Omega}\sum_i \left[q_i\vec{\tau}_i - \sum_j\sum_{\xi\xi'} w^{j,1}_{i,\xi\xi'}\vec{d}^{1}_{i,\xi'\xi} - \sum_j\sum_l \Delta\left(\tilde{c}^{j}_{il}\right)^2\vec{R}_l \right]. \tag{36}$$

TABLE I. Born effective charges of atoms in $BaTiO_3$ (upper table) and $PbTiO_3$ (lower table) and the contributions from each valence band. "Residual" denotes the contribution from the rest of the system excluding the valence states. For each atom, the upper figure for the cubic phase and the lower figure for the tetragonal phase. "Av. resid." denotes the average of the upper and lower figures for residual. The last column shows the corresponding ion-core charge of residual.

$BaTiO_3$	Total	O-2s	Ba-5p	O-2p	Residual	Av. resid.	Ion core
Ba	2.731	0.599	−7.050	1.225	7.957	7.959	8
	2.830	0.618	−7.053	1.302	7.962		
Ti	7.319	0.201	0.282	2.939	3.896	3.842	4
	5.672	0.219	0.307	1.358	3.788		
O1, O2	−2.135	−2.177	0.420	−6.364	5.986	5.987	6
	−1.952	−2.191	0.422	−6.171	5.987		
O3	−5.781	−2.446	−0.071	−9.439	6.175	6.222	6
	−4.636	−2.454	−0.097	−8.353	6.269		
$PbTiO_3$	Total	O-2s	Pb-5d	Pb-6s	O-2p	Residual	Av. resid.	Ion core
Pb	3.895	3.074	−12.910	−3.573	3.281	14.023	14.029	14
	3.487	−0.525	−9.459	−3.466	2.902	14.035		
Ti	7.191	0.007	0.301	0.622	2.433	3.828	3.694	4
	5.097	1.551	−1.148	1.298	−0.165	3.561		
O1, O2	−2.596	−3.395	1.405	0.591	−7.178	5.981	5.986	6
	−2.106	−1.831	−0.106	0.450	−6.610	5.991		
O3	−5.896	−2.291	−0.201	−0.231	−9.360	6.187	6.300	6
	−4.388	−3.353	0.808	−0.718	−7.538	6.413		

Obviously the following charge neutrality condition

$$\sum_i q_i = 0 \tag{37}$$

is satisfied.

If we take account of contributions to the polarization from sufficiently deep semicore states, the residual Born effective charge Z_i^r is well approximated by the corresponding ion-core charge which can be obtained by simply counting the number of valence electrons. Table I shows the contribution to the Born effective charge from each valence or semicore state for $BaTiO_3$ and $PbTiO_3$. Clearly the residual Born effective charges Z_i^r are nearly equal to the ion-core charges with some appreciable deviation for Ti and O3. If we include Ti-3p states as semicore states, Z_i^r for Ti and O3 will become much closer to the ion-core charges [8].

III. MECHANISM OF ELECTRONIC POLARIZATION

We first explain how the third and fourth terms of Eq. (23) are related to the physical processes by considering the hybridized bands formed by A atom and B atom aligned along a linear chain in a ferroelectric material. Then we show the interdependence between the third term and the fourth term in an intuitive way.

The basic idea of the present argument follows Harrison's bond order model [8,9]. For simplicity we assume that atom A (B) has one valence state a (b) and that level a is deeper than level b. Figure 1 shows the local density of states (LDOS) of the A and B atoms in the paraelectric phase (upper) and the ferroelectric phase (lower). In the latter phase, atoms B are displaced as shown by blue arrows. With such atomic displacement, the a-b hybridization for the B1-A2 pair is strengthened. Then the B1 component increases in band a and the A2 component increases in band b. For pairs A1-B1 and A2-B2, the a-b hybridization is weakened and the change in each component in each band is reversed. Therefore, in band a, associated with the phase change from paraelectric to

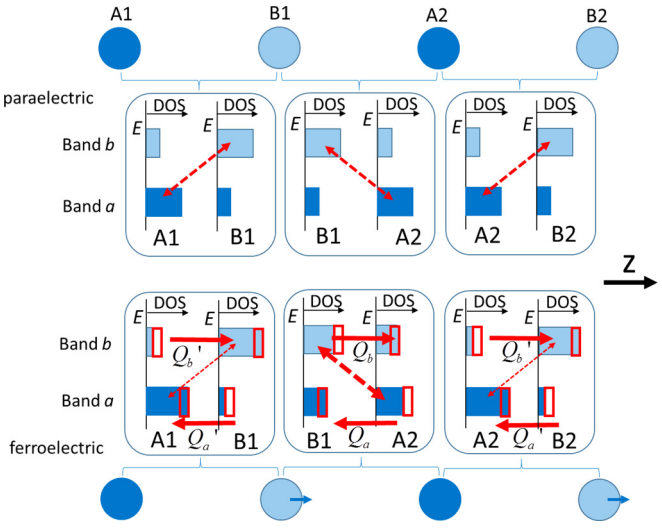

FIG. 1. (Color online) Mechanism for the electronic polarization induced by the atomic displacement. The upper half is for the paraelectric phase and shows the schematic density of states of the AB compound in which the a state of atom A has a lower energy than the b state of atom B. The red broken arrows show the a-b hybridization. The lower half shows the case of the ferroelectric phase. The pair with a shortened (elongated) atomic distance has stronger (weaker) hybridization. The change in the hybridization induces the electron transfer indicated by the horizontal red arrows. The leftward (rightward) electron transfer produces positive (negative) polarization.

ferroelectric, electrons are transferred from A2 to B1 for the B1-A2 pair, from B1 to A1 for the A1-B1 pair, and from B2 to A2 for the A2-B2 pair. The spatial direction of the electron transfer in band a is leftward as is shown by left-pointing red arrows in Fig. 1. The situation is reversed in band b. The net polarization associated with the electron transfer is zero if both a and b bands are occupied. If only band a is occupied, the leftward electron transfer will produce the rightward polarization. In most of the ferroelectric materials, the top of the valence band is formed mainly by anion orbitals and the bottom of the conduction band by cation orbitals. In the scheme of Fig. 1, atom A is an anion and band a is the top valence band, while atom B is a cation and band b is the bottom conduction band which is empty. Therefore, the electron transfer within band a produces the polarization in the direction of the cation displacement. On the other hand, we pointed out that the top valence band of TTF-CA is dominated by the TTF(cation)-HOMO and that the bottom conduction band by the CA(anion)-LUMO [15]. In such a case, B in Fig. 1 is CA (anion) and A is TTF (cation). Then, the polarization produced by the electron transfer is parallel to the anion displacement. This explains the puzzling feature of TTF-CA that the electronic polarization and the ionic one are in the opposite direction.

We make comments on the relation between the local density of states and the MLWO and explain the relation between the polarization and the change in MLWO due to the phase change from paraelectric to ferroelectric. For example, we take the trimer B1-A2-B2 in Fig. 1 and consider the MLWO of band a. The LDOS suggests large weight of the MLWO at atom A2 and small tails at atoms B1 and B2. Associated with the phase change from paraelectric to ferroelectric, the central weight of MLWO at atom A2 changes little because the change in the A2 component LDOS for the B1-A2 pair is mostly canceled by that for the A2-B2 pair. However, as for the tail part, weight is reduced at B2 and enhanced at B1. This suggests that the shift of the WFC corresponding to the polarization is dominated by the transfer of the tail part from B2 to B1 as pointed out before [8,12]. As for band b, we take the trimer A1-B1-A2. Then the displacement of B atoms produces the transfer of the tail part of the b band MLWO from A1 to A2. Such behaviors can be actually seen in the MLWOs of the O-2p bands (band a) and Ti-3d bands (band b) in $PbTiO_3$ and also those of the TTF and Ca bands in TTF-CA as shown in Figs. 2 and 3. Similar results were shown in Fig. 4 in Ref. [12]. These processes of the tail-part transfer correspond to the fourth term (electron flow term) of Eq. (23). We can also understand that the electron flow in band a (b) is mostly contributed by the b (a) orbitals.

The electron transfer processes in band a of Fig. 1 is reproduced in a simplified manner in Fig. 4, with $Q'_a = Q_a - \delta q$. [In Fig. 4 the amount of transferred charge given by Q_a (and $Q_{a'}$, δq) multiplied by the electron charge $-e$ is shown.] When atoms are displaced by a small amount proportional to $\delta\lambda$ from the symmetric paraelectric phase ($\lambda = 0$), δq must be of the order of $(\delta\lambda)^2$ if the lattice does not deform. However, if atoms are displaced with reference to an already displaced configuration ($\lambda \neq 0$), the asymmetry of the reference produces δq of the order of $\delta\lambda$. Generally we can expect that $\delta q > 0$.

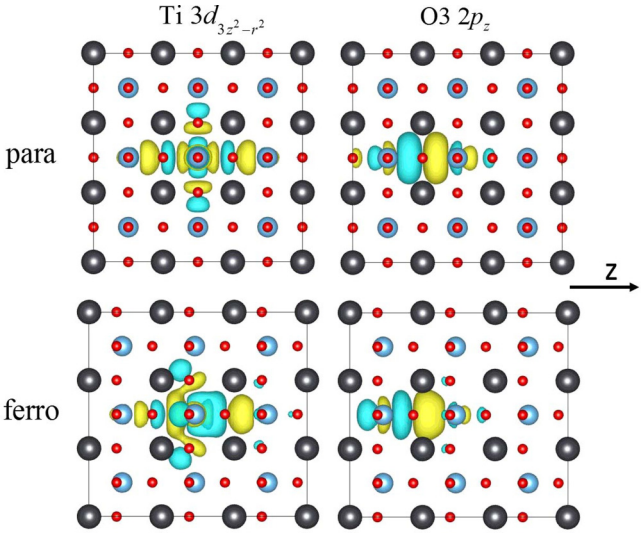

FIG. 2. (Color online) The left two are the $3z^2 - r^2$ type MLWO of the Ti-3d conduction band and the right two are the p_z type MLWO of the O-2p valence band for $PbTiO_3$. The upper (lower) panel is for the paraelectric (ferroelectric) phase. Oxygen atoms displace leftward in the ferroelectric phase. In the background lattice, large black spheres are Pb and small red spheres are O. Ti is hidden by O or wave function. The yellow (blue) part is the positive (negative) part of the MLWO.

The electron transfer shown in Fig. 4(a) is equivalent to that in Fig. 4(b). The broken rectangle represents the unit cell and atom A2 at the boundary is taken to be a member belonging to this unit cell in Fig. 4(b). Figure 4(b) clearly explains that the electron transfer between B atoms in neighboring unit cells corresponds to the fourth term of Eq. (23) and the electron transfer between A and B atoms within a unit cell the third term of Eq. (23). However, the third term and the fourth term are not independent as can be easily understood by comparing Figs. 4(b) and 4(c). The electron transfer shown in Fig. 4(a) is also equivalent to that in Fig. 4(c), where atom A3 in the

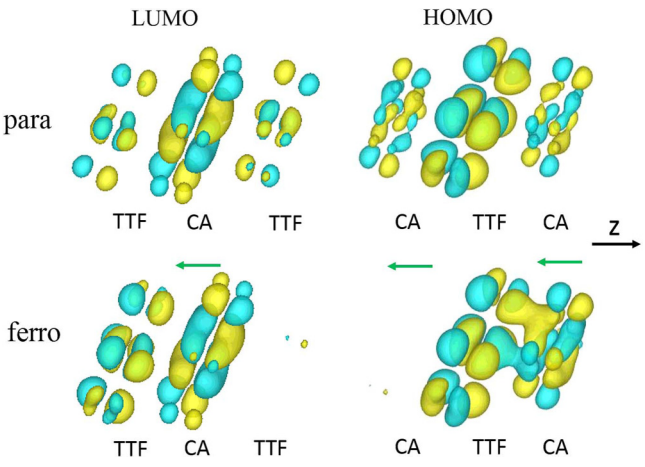

FIG. 3. (Color online) The left two are the MLWOs of the LUMO band and the right two are those of the HOMO band for TTF-CA. The upper (lower) panel is for the paraelectric (ferroelectric) phase. In the ferroelectric phase, CA displaces leftward as indicated by green arrows. The yellow (blue) part is the positive (negative) part of the MLWO.

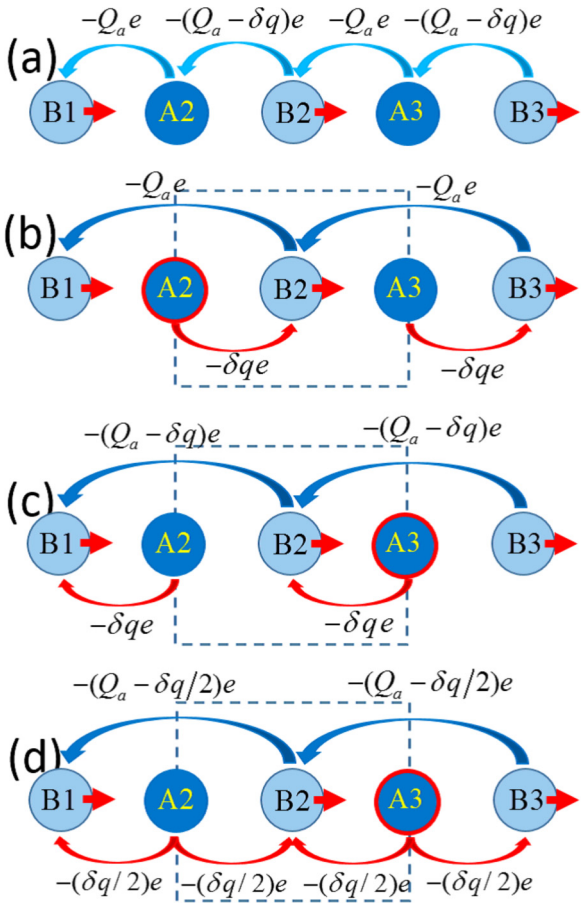

FIG. 4. (Color online) (a) The electron transfer shown in the lower panel of Fig. 1. Here and also in the following, the transferred charge ($-e\times$ amount of electron transfer) is shown. (b) The electron transfer shown in (a) can be converted to a scheme having a combination of the electron flow and the electron transfer within a unit cell. (c) Another possible scheme equivalent to scheme (b). (d) A more appropriate picture for the electron transfer in bulk systems.

right side of the boundary is taken to be a member of the unit cell. In other words, the basis vector of atom B is changed by a lattice constant and the difference in the third term due to the change of the basis vector can be merged into the fourth term. We solve this ambiguity by pointing out that the contribution from the electron transfer between atoms within a unit cell should not be present in the periodic bulk system. Therefore, an intuitively understandable picture in the bulk system, more appropriate than Figs. 4(b) and 4(c), is shown in Fig. 4(d), where the electron transfer from A atoms to B atoms occurs in both ways with a modified amount of charge for the electron flow contribution.

IV. COMPUTATIONAL DETAILS

In order to calculate electronic structures and MLWOs of target materials, we used our computational code QMAS (quantum materials simulator) [23], which is based on the projector augmented-wave (PAW) method [24] and the plane-wave basis set with the generalized gradient approximation (GGA) [25] for the exchange-correlation energy. To describe the ferroelectric and the reference paraelectric phases, we used experimental structural data for $BaTiO_3$ (a ferroelectric tetragonal structure [26] and a paraelectric cubic structure [27]), for $PbTiO_3$ (a ferroelectric tetragonal structure and a paraelectric cubic structure [28]), and for TTF-CA (a 40 K ferroelectric and a 90 K paraelectric structures [29]). Detailed structural information for the former two compounds is given in Table S1 of the Supplemental Material [22]. We interpolated the structures with $\lambda = 0$ and $\lambda = 1$ linearly for each material and made calculations for interpolated structures with intermediate λ values also. The plane-wave energy cutoff was set to 20.0 hartrees. The number of $\boldsymbol{k}$ points for self-consistent calculations was set, in the full Brillouin zone, to $8 \times 8 \times 4$ for TTF-CA and to $8 \times 8 \times 8$ for $BaTiO_3$ and $PbTiO_3$. When constructing MLWOs and making further analyses, with the self-consistent charge fixed, we performed additional calculations on the $\boldsymbol{k}$ point mesh of $8 \times 8 \times 4$ for TTF-CA and on that of $12 \times 12 \times 12$ for $BaTiO_3$ and $PbTiO_3$. The polarization values were obtained by the Berry's phase approach [1,2]. Details of the selection of valence bands and conduction bands in the present formulation will be described later in each application. To illustrate MLWOs, we used the 3D visualization program VESTA [30].

V. APPLICATIONS

A. TTF-CA

We explained the exotic ferroelectric properties of TTF-CA by calculating the Born effective charges and analyzing them by using the formulation developed in this work [15]. We also presented a physical picture for the mechanism of producing the electronic polarization in the opposite direction to that of the ionic polarization in contrast to most of other ferroelectric materials. Here we give supplementary information and discussion about the electronic polarization of TTF-CA.

In the TTF-CA crystal there are two columns along which TTF and CA are stacked alternately and the unit cell has two pairs of TTF and CA. They are parallel to the crystal a axis along which the net electric polarization is observed. As the two columns interact very weakly, the system has strong one-dimensional character. We can neglect the effects of the interchain interaction in the discussion of the electric polarization, although they are taken into account in the actual electronic structure calculations for the Berry's phase estimation of the polarization and the calculation of MLWOs [31]. If we neglect the interchain interaction, $n_v = 1$ for the TTF-HOMO dominating valence band, $n_c = 1$ for the CA-LUMO dominating conduction band, and $n_{vc} = n_v + n_c = 2$ in the formulation of Sec. II. As we have only one valence band, the superscript j in Eq. (36) is not shown in this subsection. Because the top valence band is a bonding state between TTF-HOMO and CA-LUMO, TTF donates electrons to CA, making TTF a cation and CA an anion. Here we note again that the cation level is the highest below the Fermi level and that the anion level is the lowest above the Fermi level in TTF-CA, which is in sharp contrast to the energy diagram of TMO. This is the reason why the electronic polarization is in the opposite direction to the ionic polarization in TTF-CA [15].

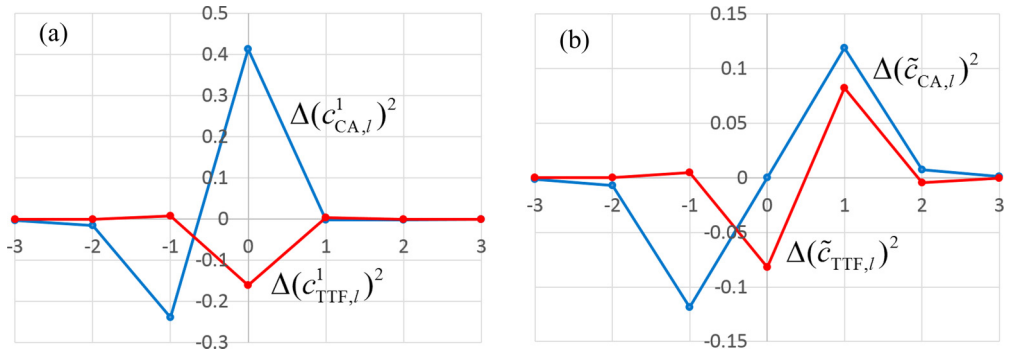

FIG. 5. (Color online) (a) The original expansion coefficients for CA and TTF for $\lambda = 1$ versus the lattice points. (b) Those defined by Eqs. (38) and (39).

In the present system $\Delta(c^{-1}_{il})^2$ can be easily related to $\Delta(c^1_{il})^2$ and then all the terms of Eq. (36) can be expressed in terms of the expansion coefficients for $\lambda = 1$. Following the prescription in the Supplemental Material [22] we obtain

$$\Delta(\tilde{c}_{\mathrm{CA},l})^2 = \tfrac{1}{2}\left[\Delta\left(c^1_{\mathrm{CA},l}\right)^2 - \Delta\left(c^1_{\mathrm{CA},-(l-1)}\right)^2\right] \tag{38}$$

and

$$\Delta(\tilde{c}_{\mathrm{TTF},l})^2 = \tfrac{1}{2}\left[\Delta\left(c^1_{\mathrm{TTF},l}\right)^2 - \Delta\left(c^1_{\mathrm{TTF},-l}\right)^2\right]. \tag{39}$$

The above equations correspond to a case where a CA molecule is put at the origin of the unit cell. As there are two pairs of TTF and CA, the explicit expression of the polarization is given by

$$\Delta\vec{P} = \frac{2e}{\Omega}\left[\{q_{\mathrm{CA}}\vec{\tau}_{\mathrm{CA}} + q_{\mathrm{TTF}}\vec{\tau}_{\mathrm{TTF}}\} - \left\{w^1_{\mathrm{CA}}\vec{d}^1_{\mathrm{CA}} + w^1_{\mathrm{TTF}}\vec{d}^1_{\mathrm{TTF}}\right\} - \sum_l \left\{\Delta(\tilde{c}_{\mathrm{CA},l})^2 + \Delta(\tilde{c}_{\mathrm{TTF},l})^2\right\} l\vec{a}\right], \tag{40}$$

with $\vec{a}$ denoting the unit cell lattice vector along the TTF-CA chain and the local molecular charges in the ferroelectric phase defined by

$$q_{\mathrm{CA}} = -w^1_{\mathrm{CA}} \tag{41}$$

TABLE II. The contribution from each term to the polarization of Eq. (36) for TTF-CA, $BaTiO_3$, and $PbTiO_3$. The total polarization estimated by the Berry's phase approach is given in the bottom line. Units in $\mu C/cm^2$.

	TTF-CA	$BaTiO_3$	$PbTiO_3$
PCM[a]	0.26	10.22	31.26
LP[b]	∼0.0	0.10	11.25
EF[c]	−10.14	22.31	54.58
$\Delta P_{\mathrm{total}}$	−9.88	32.63	97.09
Berry's phase			
$\Delta P_{\mathrm{total}}$	−10.0	32.37	97.14

[a]PCM: point-charge model.
[b]LP: local polarization.
[c]EF: electron flow.

and

$$q_{\mathrm{TTF}} = 2 - w^1_{\mathrm{TTF}}. \tag{42}$$

In the present case, only one molecular orbital is taken into account for each of TTF and CA and the population matrix and dipole tensor are both diagonal. Anyway, although the TTF and CA molecules deform slightly in the ferroelectric phase, the molecular dipole moment of Eq. (22) can be neglected in the polarization [18].

In the present work we displace CA along $-\vec{a}$ because this choice of the sign for the anion displacement is common in most of the works on ferroelectrics and makes the sign of the PCM contribution positive. However, as CA was displaced along $\vec{a}$ in our previous works [15,31], the sign of the polarization was opposite to the one in this paper. The l dependencies of $\Delta(c^1_{\mathrm{CA},l})^2$ and $\Delta(c^1_{\mathrm{TTF},l})^2$ are shown in Fig. 5(a). From this result we retained only $\Delta(c^1_{\mathrm{CA},0})^2$, $\Delta(c^1_{\mathrm{TTF},0})^2$, and $\Delta(c^1_{\mathrm{CA},-1})^2$ as a first approximation in our previous work [15]. We also considered a case with $\vec{\tau}_{\mathrm{TTF}} = 0$ because it was nearly the case in our earlier work [31]. Then the polarization was estimated to be −9.2 to −9.4 $\mu C/cm^2$ [32].

The modified electron-flow terms given by Eqs. (38) and (39) are shown in Fig. 5(b). The larger l components are enhanced due to another factor of l. If we take into account the contributions from $l = -2$ to $+2$ in the last term of Eq. (40) together with the displacements of CA and TTF [33], the polarization is given as -9.88 $\mu C/cm^2$. This agrees quite well with the corresponding value -10.0 $\mu C/cm^2$ obtained by the Berry's phase approach [31]. Therefore, the polarization coming from the top valence band governs almost entirely the total polarization in TTF-CA. We used the following structural data of $|\vec{a}| = 7.2$ Å, $\Omega = 7.74 \times 10^2$ Å^3, $\tau_{\mathrm{CA}} = -0.076$ Å, and $\tau_{\mathrm{TTF}} = 0.007$ Å. The latter two values are those used in our earlier work (with the sign change) [31]. These structural data give $q_{\mathrm{TTF}} = -q_{\mathrm{CA}} = 0.737$ and each contribution of Eq. (40) as shown in Table II [34]. Note that the direction of the electronic contribution to the polarization is opposite to that of the ionic contribution.

Similarly to Fig. 4, the contributions to the polarization described by Eq. (40) is schematically shown in Fig. 6. Here the electron flow by a distance la via CA or TTF is given by [35]

$$Q_{i,l} = \Delta(\tilde{c}_{i,l})^2 - \Delta(\tilde{c}_{i,-l})^2, \tag{43}$$

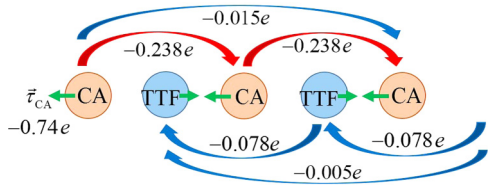

FIG. 6. (Color online) Electronic processes associated with the molecular displacement shown by green arrows. The red (blue) arrows show the major (minor) processes of electron flow. The amount of charge transfer is shown. Note that anion (CA) moves leftward producing the positive polarization, while electrons move rightward producing the negative polarization.

with i denoting either CA or TTF. The ionic displacements with green arrows give the PCM term [first term of Eq. (40)]. The major (minor) contributions in the electron flow given by Eq. (43) are shown with red (blue) arrows. Clearly the most important contribution comes from the electron flow via CA which produces negative polarization. As the valence band is governed by a TTF-HOMO component, the electron flow is mostly contributed by the counter-orbital CA-LUMO being consistent with the argument made for Fig. 1. We note that the third term in Eq. (40) makes important contributions because of the large distance of electron movement despite the small amount of electrons involved.

B. $BaTiO_3$

1. Calculation setup

In most of perovskite TMOs, the electronic polarization is mainly governed by the O-2p bands through the hybridization with the unoccupied TM-d bands. Our previous paper treated this case [16]. However, as can be seen in Fig. 22 of the review article [36], Fig. 2 of our previous paper [16] for $BaTiO_3$ and Fig. 2 of this paper for $PbTiO_3$, the deformation of MLWO of the O-2p_z state in the ferroelectric phase clearly suggests a contribution of the intra-atomic polarization through the s-p_z hybridization. Therefore, we explicitly treat O-2s bands as valence bands. Besides, as Ba-5p bands are located between O-2s and O-2p bands, they are also included in the valence bands. (The band center energies with respect to the band gap center are −16.81 eV for the O-2s bands, −10.38 eV for the Ba-5p bands, −2.42 eV for the O-2p bands, and 1.89 eV for the Ti-3d bands for the cubic phase.) These three bunches of occupied bands are treated separately in the analysis of the polarization following the prescription given in Sec. II. (To pursue higher accuracy, we should include also Ti-3p and Ba-5s states [8].) For the expansion of Eq. (7), we include the MLWOs of Ti-3d states in addition to those for the above three valence states, leading to altogether 20 basis orbitals.

While the paraelectric phase has the cubic symmetry, the tetragonal symmetry is assumed for the ferroelectric phase, which is stable at room temperature. The structural information is given in Table S1 of the Supplemental Material [22] with the Ba position taken as the reference for the atomic displacement. With the principal axis of the tetragonal symmetry along the crystal c axis, O1 and O2 are symmetrically connected in both phases and the polarization appears only along the crystal c axis, which is parallel to the global z axis.

TABLE III. Contribution from each bunch of valence bands to the polarization of Eq. (36) in $BaTiO_3$. The third line "Residual charge" denotes the PCM contribution due to the charge of each atom excluding the valence electrons. The total polarization is given by the sum of a, b and c in the last column. Units in $\mu C/cm^2$.

	O-2s band	Ba-5p band	O-2p band	Sum
PCM of Eq. (23)	8.720	0.667	20.096	29.484
Residual charge				−19.261
PCM of Eq. (36)				10.223[a]
LP	1.171	0.468	−1.542	0.097[b]
EF	1.231	−1.053	22.126	22.305[c]
Total ($a+b+c$)				32.625

[a]PCM: point-charge model.
[b]LP: local polarization.
[c]EF: electron flow.

2. Results and analysis

For the expansion of Eq. (7), the lattice points included in the summation over l are those which satisfy the condition of $1 \geqslant l_x,l_y,l_z \geqslant -1$ with the lattice points expressed as $\vec{R}_l = l_x(a,0,0) + l_y(0,a,0) + l_z(0,0,c)$. In contrast to our previous work [16] where only four lattice points were included and the left-hand side of Eq. (9) was 0.996 for the O-2p band, we include 27 lattice points to give 0.9994 as the left-hand side of Eq. (9) in the present work. Each contribution from the three terms of Eq. (36) is presented in Table II. Similarly to the case of TTF-CA, the electron-flow term makes the dominant contribution to the polarization. In order to further analyze the contents of the polarization, we show two different cross sections of Eq. (36). Although the first term includes the summation only over atoms, the other three terms are expressed in terms of the double summation over band bunches and atoms. First, we show in Table III the contributions from the second and third terms of Eq. (36) for each of the three bunches of valence bands separately by summing only over atoms. With Eq. (35), the first term of Eq. (36) can be divided into the sum of the first term of Eq. (23) over the bunches of valence bands and the contribution coming from the residual ionic charges Z_i^r. The former is shown in the second line and the latter in the last column of the third line of Table III. As the Berry's phase approach gives 32.37 $\mu C/cm^2$ as the total polarization (Table II), the present prescription gives a satisfactory result. As expected, the O-2p bands dominate the polarization. While the O-2s bands also contribute about 10% of the electronic polarization (LP + EF), the Ba-5p bands make a negligible contribution.

The second cross section obtained by first summing over band bunches gives information on the contributions from different atoms and the results are shown in Table IV. In this case the PCM term is divided into contributions from different atoms. Nevertheless, the individual atom contribution to the PCM term depends on the choice of the reference atom. Therefore, the more fundamental quantity for the PCM term is the atomic charge given by Eq. (35), which is shown in Table S2 of the Supplemental Material [22] together with the number of valence electrons given by Eq. (20) and the residual Born effective charge of Eq. (34). In contrast to the PCM term, the second (LP) and the third (EF) terms depend on the relative

TABLE IV. Contribution from each atom to the polarization of Eq. (36) in $BaTiO_3$. Units in $\mu C/cm^2$.

Eq. (36)	O1	O2	O3	Ba	Ti	Sum
PCM	1.502	1.502	2.730	0.000	4.489	10.223[a]
LP	0.476	0.476	−1.587	0.547	0.185	0.097
EF	−0.699	−0.699	−0.965	1.538	23.069	22.305
LP + EF	−0.223	−0.223	−2.552	2.085	23.254	22.402[b]
Total ($a+b$)						32.625

[a]PCM: point-charge model.
[b]LP: local polarization, EF: electron flow.

position of atoms. Therefore, as a measure of the contribution from each atom, we show the partial sum of (LP + EF) in the second bottom line of Table IV. It is rather striking to find that the contribution from Ti is predominant in the polarization. This is because the electronic polarization in the O-2p bands is mostly determined by the electron flow which is carried by the unoccupied Ti-3d orbitals [12].

By using the calculated $\Delta(c^{\lambda}_{i\xi l})^2$, we can analyze the detailed electronic processes in the polarization for each bunch of valence bands. Similarly to Eq. (43), the amount of electrons Q_i^j in the jth bunch of valence bands transferred via atom i in the *positive* z direction by the lattice constant c is given by

$$Q_i^j = \sum_{l_x}\sum_{l_y}\left[\Delta\left(\tilde{c}^j_{i(l_x l_y 1)}\right)^2 - \Delta\left(\tilde{c}^j_{i(l_x l_y \bar{1})}\right)^2\right]. \qquad (44)$$

The results are shown by arrows in Fig. 7 [the red (blue) ones for the major (minor) contributions]. For a negative Q_i^j, the direction of the arrow is in the negative z direction. (Note that in these figures the amount of transferred charge $-|Q_i^j|e$ is shown.) We can also analyze what orbitals of atom i contribute to Q_i^j by using Eq. (17). Clearly in Fig. 7 the electron flow carried by Ti-3d orbitals dominates the polarization. In this process, the $pd\pi$ hybridization between O3-2p_x (2p_y) and Ti-3d_{zx} (3d_{yz}) makes even larger contribution than the $pd\sigma$ hybridization between O3-2p_z and Ti-3$d_{3z^2-r^2}$ as discussed before [10,12]. The situation can also be clearly seen in the MLWOs of O3-2p states. (See Fig. 2 of our previous paper [16] and also Figs. S11(g)–S11(i) of the Supplemental Material [22]. Similar results for $PbTiO_3$ in Figs. S23(g)–S23(i).)

Some more details seen in Fig. 7 are as follows. The rightward electron flow carried by O3 in the O-2p bands produces a negative contribution to the polarization through electron-flow shown in Table IV. Similarly, a positive electron-flow contribution by Ba in Table IV is due to the electron flow carried by Ba in the O-2p and 2s bands. In the O-2p bands, the electron-flow contributions through Ba and O3 nearly cancel out.

For the electronic processes in the Ba-5p bands, the dominant contribution is the rightward electron flow carried by O1 and O2 which produces a negative electronic polarization in Table III. This negative contribution is partly canceled by a positive contribution due to the electron flow through Ti and the net polarization in the Ba-5p bands is quite small.

The 2s states at O1 and O2 hybridize with Ba-5p states and produce the electron flow through Ba-5p orbitals as shown in right panel of Fig. 7. On the other hand, the 2s state at O3 hybridizes with the Ti-3$d_{3z^2-r^2}$ state and this hybridization produces the positive electron-flow contribution seen in Table III. The relation between Ba-5p bands and O-2s bands corresponds qualitatively to the situation shown in Fig. 1, with O-2s bands as band a and Ba-5p bands as band b. However, as O-2s bands hybridize also with Ti-3d bands and Ba-5p bands hybridize also with O-2p bands, the Ba-5p and O-2s bands do not form a closed set of bands.

The net contribution from the local polarization is negligible, while the effect in each band and/or atom is not so small. Here we only point out that the hybridization between O-2s and O-2p_z produces positive polarization in the O-2s bands and a negative one in the O-2p bands. Such

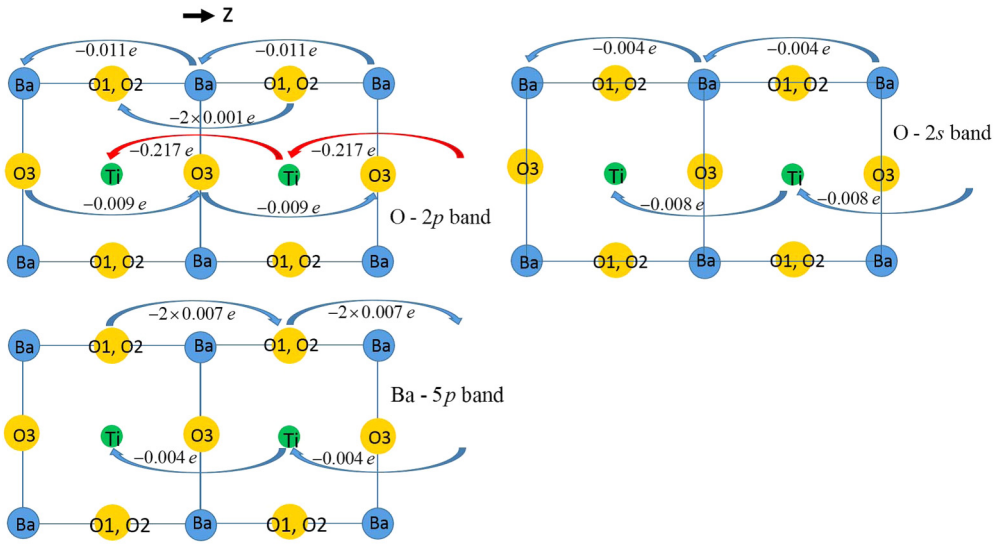

FIG. 7. (Color online) The red (blue) arrows show the major (minor) electron-flow processes in $BaTiO_3$. The upper left for O-2p band, the lower left for Ba-5p band, and the right for O-2s band. Amount of transferred charge is shown. The rightward (leftward) arrows produce the negative (positive) polarization.

TABLE V. Contribution from each bunch of valence bands to the polarization of Eq. (36) in $PbTiO_3$. The third line "Residual charge" denotes the PCM contribution due to the charge of each atom excluding the valence electrons. The total polarization is given by the sum of a, b and c in the last column. Units in $\mu C/cm^2$.

	O-2s band	Pb-5d band	Pb-6s band	O-2p band	Sum
PCM of Eq. (23)	68.366	8.162	7.519	200.814	284.861
Residual charge					−253.606
PCM of Eq. (36)					31.256[a]
LP	2.752	0.097	−0.174	8.578	11.253[b]
EF	26.810	−24.443	−18.894	71.107	54.579[c]
Total ($a+b+c$)					97.088

[a]PCM: point-charge model.
[b]LP: local polarization.
[c]EF: electron flow.

cancellation is expected because both O-2s and O-2p states are occupied.

C. $PbTiO_3$

1. Calculation setup

In comparison to Ba in $BaTiO_3$, Pb in $PbTiO_3$ has much lower 6s and 6p levels so that the Pb-6s band is occupied and located below the O-2p bands and 6p bands are located just above the Ti-3d bands with some overlap. The Pb-6s and 6p states hybridize strongly not only with the O-2p states [28,37] but also with each other to produce large local polarization. In addition to this, we include O-2s states and also Pb-5d states because the energy of the Pb-5d states is just above that of the O-2s state. (The band center energies with respect to the band gap center are −17.07 eV for the O-2s bands, −16.44 eV for the Pb-5d bands, −6.81 eV for the Pb-6s band, −2.36 eV for the O-2p bands, 1.75 eV for the Ti-3d bands, and 3.33 eV for the Pb-6p bands for the cubic phase.) The number of valence states is 18 and the number of basis orbitals is 26 (including the Pb-6p orbitals). The ferroelectric phase has the tetragonal symmetry and the polarization appears only along the crystal c axis. The Pb position is taken as the reference for the atomic displacement.

2. Results and analysis

The lattice points included in the expansion of Eq. (7) are the same as those for $BaTiO_3$ and the left-hand side of Eq. (9) is 0.9986 for the O-2p bands of $PbTiO_3$. Each contribution from the three terms of Eq. (36) is presented in Table II. Compared to the case of $BaTiO_3$, $PbTiO_3$ has roughly three times larger polarization partly due to the larger atomic displacements. In the following, we will analyze the details of the difference between $BaTiO_3$ and $PbTiO_3$.

Similarly to $BaTiO_3$, we show two different cross sections of Eq. (36) in Tables V and VI. Detailed electronic processes are shown in Figs. S1 and S2 in the Supplemental Material [22] for the four bunches of valence bands. In these tables and figures we used the local charge of each atom listed in Table S3. First we point out characteristic features of $PbTiO_3$ by comparing Tables V and VI with Tables III and IV. For $PbTiO_3$, all four bunches of valence bands make significant contributions to the polarization. The contribution from the O-2s bands is an order of magnitude larger for $PbTiO_3$ than for $BaTiO_3$ and the Pb bands also make a much larger contribution than the Ba bands. These features are the results of the stronger hybridization between the O states and the Pb states [28,37]. As the O-2s bands and the Pb-5d bands are energetically close, these bands form roughly a closed system as shown schematically in Fig. 1. Therefore, the two contributions from the O-2p bands and the Pb-5d bands cancel significantly with only about 5.2 $\mu C/cm^2$ as a net electronic contribution (LP + EF), which may be assigned as a contribution coming from the hybridization between the O-2s bands and the Ti-3d bands. The large negative contribution from the Pb-6s band is also mostly due to the hybridization with the O-2p bands.

The mechanism of the negative polarization in the Pb-5d bands and the Pb-6s band is schematically shown in Fig. 8. The upper panel of Fig. 8 which corresponds to the O-2s and Pb-5d band complex is basically the same as the lower panel of Fig. 1, except the mode of the atom displacement. In Fig. 8, instead of displacing atom B in Fig. 1, atom A is displaced in the opposite direction to be consistent with the choice of Pb as the reference atom. For the O-2p and Pb-6s band complex, Fig. 1 is modified slightly to give the lower panel of Fig. 8, where the Pb-6s band is deeper than the O-2p bands. The two panels in Fig. 8 show that in both the Pb-5d and Pb-6s bands, electrons move from left to right so that the resulting polarization is directed to the left (negative polarization). On the other hand, the polarization in the O-2s and O-2p bands caused by the hybridization with the Pb-5d and Pb-6s states is positive. These figures also show that the electron-flow contributions in the Pb bands are mediated by the O orbitals and vice versa.

These features are clearly correlated with the changes in MLWOs for O1 (equivalent to O2) and Pb as shown in Figs. 9 and 10. In both O-2s and O-2p bands (Fig. 9), the weight of

TABLE VI. Contribution from each atom to the polarization of Eq. (36) in $PbTiO_3$. Units in $\mu C/cm^2$.

Eq. (36)	O1	O2	O3	Pb	Ti	Sum
PCM	15.079	15.079	9.526	0.000	−8.427	31.256[a]
LP	0.152	0.152	−1.104	11.339	0.713	11.253
EF	−21.510	−21.510	−1.385	64.237	34.747	54.579
LP + EF	−21.358	−21.358	−2.489	75.577	35.460	65.832[b]
Total ($a+b$)						97.088

[a]PCM: point-charge model.
[b]LP: local polarization, EF: electron flow.

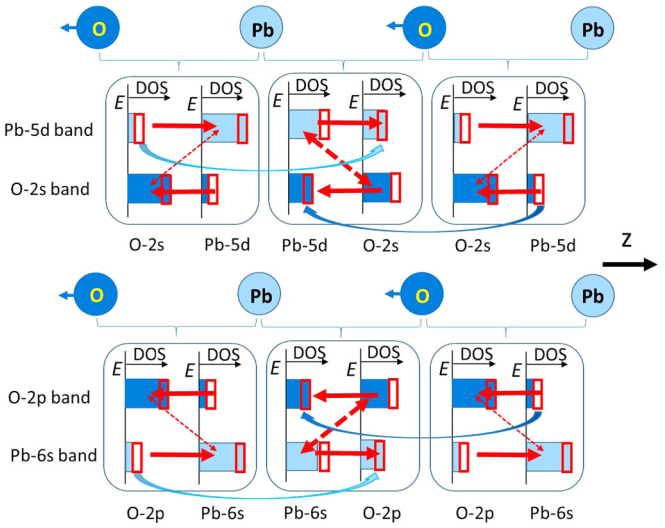

FIG. 8. (Color online) Schematic explanation on the mechanism of the polarization in the Pb-5*d* and O-2*s* band complex (upper panel) and in the O-2*p* and Pb-6*s* band complex (lower panel). In both band complexes, the direction of the electron transfer is rightward in the Pb bands, producing the negative polarization while, that in the O bands is leftward producing the positive polarization. The light blue and dark blue curvy arrows indicate the electron flow processes.

the tail of MLWO is transferred from the right Pb sites to the left Pb ones producing large positive contributions of Pb to the polarization through not only the electron flow but also the local polarization [12]. On the other hand, in both Pb-5*d* and Pb-6*s* bands (Fig. 10), we find similar weight transfer occurs at O sites from left to right producing negative contributions of O sites to the polarization. The contribution from each atom to the polarization is shown in Table VI. Similarly to the case of $BaTiO_3$, Ti makes a large positive contribution. However, it

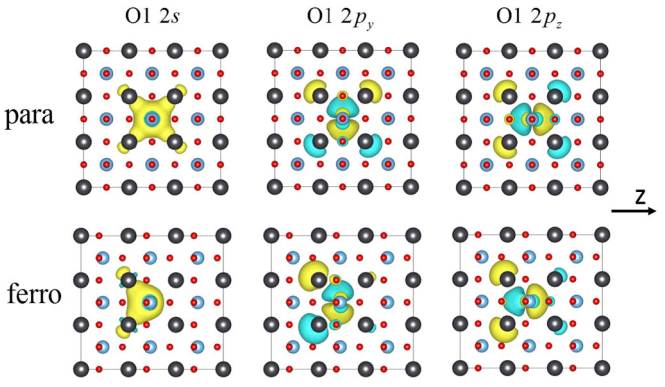

FIG. 9. (Color online) Examples of the MLWOs with their center at O1 of $PbTiO_3$. The left side shows those of the O-2*s* bands and the middle and right sides are for those of the O-2*p* bands. The upper panel (lower) is for the paraelectric (ferroelecteric) phase. The changes in MLWOs associated with the ferroelectric transition produce the electron flow contributions to the polarization via Pb orbitals. At the same time, the appearance of the net intra-atomic polarization at the Pb sites can also be seen. In the background lattice, large black spheres are Pb and small red spheres are O. Ti is hidden by O or wave function. The yellow (blue) part is the positive (negative) part of the MLWO.

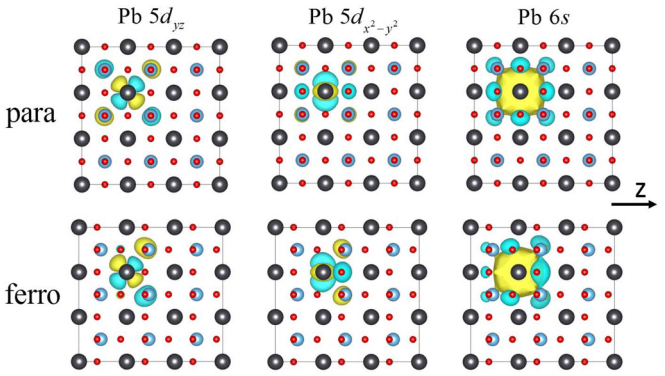

FIG. 10. (Color online) Examples of the MLWOs with their center at Pb of $PbTiO_3$. The left and middle sides show those of the Pd-5*d* bands and the right side is for those of the Pb-6*s* bands. The upper panel (lower) is for the paraelectric (ferroelecteric) phase. The changes in MLWOs associated with the ferroelectric transition produce the electron flow contributions to the polarization via O orbitals. In the background lattice, large black spheres are Pb and small red spheres are O. Ti is hidden by O or wave function. The yellow (blue) part is the positive (negative) part of the MLWO.

is rather striking to find that about a twice larger contribution comes from Pb. More detailed discussion on the electronic processes are given in the Supplemental Material [22] by presenting electron-flow diagrams in Figs. S1 and S2.

VI. CONCLUDING REMARKS

We presented a formulation to analyze the mechanism of electronic contributions to the polarization within the framework of the maximum localized Wannier orbitals (MLWO) and applied it to three typical systems, TTF-CA, $BaTiO_3$, and $PbTiO_3$. Our formulation is basically the same as the one by Bhattacharjee and Waghmare [12] but we give an expression [Eq. (36)] for the polarization which is more explicit than theirs. The expression contains three terms: the first corresponds to the point charge model, the second the local polarization, and the third the electron flow from cell to cell. As shown in Table II, the electron-flow term amounts to more than 100% for TTF-CA, 68% for $BaTiO_3$, and 56% for $PbTiO_3$ of the total polarization.

For TTF-CA, the electronic polarization is in the opposite direction to that of the ionic polarization as seen in Table II. This aspect was discussed in our previous paper [15] and also in Sec. III of the present paper. For $BaTiO_3$ and $PbTiO_3$, we demonstrated the usefulness of the present formulation by showing the two different cross sections of Eq. (36). One is the decomposition of the total polarization into the contributions from different valence bands and the other is the decomposition into the contributions from different atoms in the unit cell. In parallel to such decomposition, we showed detailed electronic processes of the polarization in each bunch of valence bands.

ACKNOWLEDGMENTS

The authors are grateful to Dr. H. Shinaoka, Dr. T. Kosugi, and Dr. T. Miyake for their cooperation in implementing the Wannier function technique to QMAS. The present work is

partly supported by Grant-in-Aid for Scientific Research (No. 22104010), the Strategic Programs for Innovative Research (SPIRE), MEXT, and the Computational Materials Science Initiative (CMSI), Japan.

[1] R. D. King-Smith and D. Vanderbilt, Phys. Rev. B **47**, 1651 (1993).

[2] R. Resta, Rev. Mod. Phys. **66**, 899 (1994).

[3] K. M. Rabe and P. Ghosez, in *Physics of Ferroelectrics*, edited by K. Rabe, Ch. H. Ahn, and J.-M. Triscone (Springer, Berlin, 2007).

[4] R. Resta, M. Posternak, and A. Baldereschi, Phys. Rev. Lett. **70**, 1010 (1993).

[5] W. Zhong, R. D. King-Smith, and D. Vanderbilt, Phys. Rev. Lett. **72**, 3618 (1994).

[6] P. Ghosez, X. Gonze, and J.-P. Michenaud, Ferroelectrics **153**, 91 (1994).

[7] M. Posternak, R. Resta, and A. Baldereschi, Phys. Rev. B **50**, 8911 (1994).

[8] P. Ghosez, J.-P. Michenaud, and X. Gonze, Phys. Rev. B **58**, 6224 (1998).

[9] W. A. Harrison, *Elementary Electronic Structure* (World Scientific, Singapore, 1999), Chap. 11.

[10] N. Marzari and D. Vanderbilt, AIP Conf. Proc. **436**, 146 (1998).

[11] P. Ghosez and X. Gonze, J. Phys.: Condens. Matter **12**, 9179 (2000).

[12] J. Bhattacharjee and U. V. Waghmare, Phys. Chem. Chem. Phys. **12**, 1564 (2010).

[13] N. Marzari and D. Vanderbilt, Phys. Rev. B **56**, 12847 (1997).

[14] K. Kobayashi, S. Horiuchi, R. Kumai, F. Kagawa, Y. Murakami, and Y. Tokura, Phys. Rev. Lett. **108**, 237601 (2012).

[15] S. Ishibashi and K. Terakura, J. Phys. Soc. Jpn. **83**, 073702 (2014).

[16] K. Terakura and S. Ishibashi, *Proceedings of Computational Science Workshop 2014 (CSW2014)*, JPS Conf. Proc. **5**, 011018 (2015).

[17] X. Wang, J. R. Yates, I. Souza, and D. Vanderbilt, Phys. Rev. B **74**, 195118 (2006).

[18] In case of TTF-CA, each molecule of TTF and CA deforms slightly in the ferroelectric phase. The shift of WFC associated with such deformation of the molecular shape for TTF and CA is at most 0.1 bohr (1 bohr = 0.529 Å) along the net polarization direction and can be safely neglected. Note, however, such deformation of the molecular shape can induce a significant change in the hybridization between TTF-HOMO and CA-LUMO. See Ref. [15] in our previous work [15].

[19] R. M. Martin, Phys. Rev. B **9**, 1998 (1974).

[20] N. Nakagawa, H. Y. Hwang, and D. A. Muller, Nat. Mater. **5**, 204 (2006).

[21] R. Resta and D. Vanderbilt, Ref. [3], p. 31.

[22] See Supplemental Material at http://link.aps.org/supplemental/10.1103/PhysRevB.91.195120 for further details of crystal structures, population analysis, derivation for Eqs. (27) to (33), electronic processes and Wannier orbitals.

[23] http://qmas.jp.

[24] P. E. Blöchl, Phys. Rev. B **50**, 17953 (1994).

[25] J. P. Perdew, K. Burke, and M. Ernzerhof, Phys. Rev. Lett. **77**, 3865 (1996).

[26] G. H. Kwei, A. C. Lawson, S. J. L. Billinge, and S.-W. Cheong, J. Phys. Chem. **97**, 2368 (1993).

[27] L. H. Brixner, J. Phys. Chem. **64**, 165 (1960).

[28] Y. Kuroiwa, S. Aoyagi, A. Sawada, J. Harada, E. Nishibori, M. Takata, and M. Sakata, Phys. Rev. Lett. **87**, 217601 (2001).

[29] M. Le Cointe, M. H. Lemée-Cailleau, H. Cailleau, B. Toudic, L. Toupet, G. Heger, F. Moussa, P. Schweiss, K. H. Kraft, and N. Karl, Phys. Rev. B **51**, 3374 (1995).

[30] K. Momma and F. Izumi, J. Appl. Crystallogr. **44**, 1272 (2011).

[31] S. Ishibashi and K. Terakura, Physica B **405**, S338 (2010).

[32] Because of the use of only $C_0(\lambda)$, $A_L(\lambda)$, and $A_R(\lambda)$, Eq. (1) of Ref. [15] does not hold exactly and therefore their Eqs. (5) and (6) are not totally equivalent. The related small ambiguity in Ref. [15] leads to small ambiguity in the polarization value.

[33] In the study of the λ dependence of the polarization, we adopted the crystal structure for a given λ obtained by a linear scaling between the crystal structure in the ferroelectric phase at 40 K and the one in the paraelectric phase at 90 K. However, to calculate the polarization in the ferroelectric phase, we use the crystal structure at 40 K and use the fictitious crystal structure obtained by averaging structures for $\lambda = 1$ and $\lambda = -1$ as a paraelectric phase. In this convention, a-axis components of $\vec{\tau}_{\rm CA}$ and $\vec{\tau}_{\rm TTF}$ are 0.0763 and -0.0074 Å, respectively. These values were used in our earlier work but not mentioned in the paper [31].

[34] The value of $q_{\rm TTF}(=-q_{\rm CA})$ in our previous work [15] is 0.75. This is slightly different from the present value because of the approximation of retaining only $c^{\lambda}_{{\rm CA},0}$, $c^{\lambda}_{{\rm TTF},0}$, and $c^{\lambda}_{{\rm CA},-1}$ in the work.

[35] $Q_{i,l}$ of Eq. (43) contains two contributions: one is from 0 to l and the other from $-l$ to 0. Therefore, Eq. (43) can be also written as

$$Q_{i,l} = [\Delta(\tilde{c}_{i,l})^2 - \Delta(\tilde{c}_{i,0})^2] + [\Delta(\tilde{c}_{i,0})^2 - \Delta(\tilde{c}_{i,-l})^2]. \quad (45)$$

[36] N. Marzari, A. A. Mostofi, J. R. Yates, I. Souza, and D. Vanderbilt, Rev. Mod. Phys. **84**, 1419 (2012).

[37] R. E. Cohen, Nature (London) **358**, 136 (1992).